Indonesian Journal of Electrical Engineering and Computer Science
Vol. 42, No. 2, May 2026, pp. 349~368
ISSN: 2502-4752, DOI: 10.11591/ijeecs.v42.i2.pp349-368

Enhancing NICD and NIMH batteries charging efficiency: a MSCCC strategy using artificial intelligence control

Somendra Banerjee, Awdhesh Kumar, Vinod Kumar Giri
Department of Electrical Engineering, Madan Mohan Malaviya University of Technology (MMMUT), Gorakhpur, India

Article Info

Article history:

Received Dec 3, 2025
Revised Mar 19, 2026
Accepted May 26, 2026

Keywords:

Adaptive neuro-fuzzy inference system
Battery management system
Constant current- constant
NiCD battery
NiMH battery
State-of-charge
Voltage (CC-CV)

ABSTRACT

In the above essay, a smart multi-stage constant current charging (MSCCC) strategy has been proposed with an adaptive neuro-fuzzy inference system (ANFIS) to improve the charging efficiency of nickel metal hydride (NiMH) and nickel cadmium (NiCd) type batteries. The suggested charger uses a boost converter that is power-factor-corrected and variable current regulation according to real-time feedback of voltage and state of charge. MATLAB/Simulink is used to test the system with a 24 V23.5 Ah NiCd pack and 25.2 V49.4 Ah NiMH pack. Comparative simulations on conventional PI, fuzzy, and neural controllers show that ANFIS-MSCCC approach enhances state-of-charge (SoC) retention by about 5-8 percent, voltage overshoot by almost 20 percent and transitions between currents are smoother which results into lower electrical stress. Besides, the suggested approach has a shorter settling time, high charging stability, and safe thermal characteristics. These findings prove that the ANFIS-aided MSCCC provides a powerful and reconfigurable charging system to NiCd and NiMH batteries, which is applicable within the complex battery management systems that are already in use.

Corresponding Author:

Somendra Banerjee
Department of Electrical Engineering, Madan Mohan Malaviya University of Technology (MMMUT)
Gorakhpur, Uttar Pradesh, India
Email: banerjeesomendra83@gmail.com

1. INTRODUCTION

Batteries that can be recharged, like nickel cadmium (NiCd) and nickel metal hydride (NiMH) ones, include becoming more and more popular in a number of industries. A NiMH battery can produce the density of energy is similar to a lithium-ion battery (LIB) in performance, and its capacity is two to three times higher than that of a NiCd battery equal in size. Degradations also occur due to a variety of factors, varying in proportion to external interaction and usage [1]. One disadvantage is that battery ageing, which occurs over the battery's lifetime, impairs performance. The four primary components of battery life and performance are temperature, recharge rate, depth of discharge, and cyclic life. Before the battery is put on the manufacturing line, it should be checked for quality for the customers. As a result, research is needed to identify devices that are deteriorating, extend their cyclic life, and determine the best charging procedure [2], [3]. Additionally, customers need to know about capacity loss, faster battery aging, and even potential battery damage [4], [5]. Typically, the manufacturer may supply the aforementioned information. It could not be adequate or certified before to installation, nevertheless. Therefore, battery quality measurement research is an essential area of study for both business and academia.

One of the most important factors in assessing a cell's energy efficiency and heat loss is its internal resistance. Battery internal resistance is intimately related to both the deterioration rate along with the

performance efficiency on the battery modules. For instance, a LIB's resistance, which changes depending on the battery's temperature, charge level, and overall health, controls its power capacity [6], [7]. As a result, numerous measuring techniques were published, including heat loss techniques, electrochemical impedance spectroscopy, and AC techniques [8].

Various current levels are used to charge using the MSCC charging technology. The two major categories into which the current level transition criteria fall are battery terminal voltage and remaining capacity separated in the literature. The next stage's current must be lower than the previous stage's current in order for this to work. Liu *et al.* [9], [10] make terminal voltage the cutoff for charge current transitions. The change dependent on voltage would be problematic If the battery is unable to be completely charged. After the last stage charge, a CV mode is frequently included to address this problem [11], [12]. While the full charge can be obtained in this manner, the cost is a longer CT and a lower CE. The state-of-charge (SoC) is used as the current transition criterion [13]-[15]. The aforementioned constraint does not apply to the present worth at each level of this standard criteria. When compared to the pulse charging technique and the CC-CV method, the SoC-based transition strategy provides lower CT and greater CE. The ant colony system (ACS) [9], Bayesian optimization [12], genetic algorithm (GA) [15], PSO [16], cuckoo optimization algorithm (COA) [17], GWO [18], and other optimization algorithms (OAs) have been used in recent years to explore the OCCP of MSCC. When compared to the CC-CV, the OA may greatly enhance the charging performance by concurrently taking into account several charging performance indicators and improving capability for searching for best solutions that meet several objectives. However, these approaches necessitate experimental validation for potential patterns of charging, which requires extensive testing and raises the time and expense of determining the best option. Furthermore, Khan and Choi [19] suggested a formula calculation approach (referred to as the FC method in this research) to ascertain the OCCP of MSCC based on the simplified ECM. The current value of each step is determined using a series of straightforward formulas. This methodology doesn't take as much time or extensive experimentation as the previously described ways. Nevertheless, it ignores the EL and TR and is solely focused on enhancing the CT. All things considered, the charge current in the CHC, CT, and EL that each stage contributes to is the main factor assessed by the MSCC charging method. Consequently, MSCC cannot proceed without first locating the OCCP.While recent investigations have examined artificial intelligence (AI)-aided multi-stage constant current charging (MSCCC) methodologies, the preponderance of published research focusses on lithium-ion batteries. Nickel-based chemistries, including NiCd and NiMH, have received comparatively less scrutiny, notwithstanding their persistent application in power tools, backup systems, and industrial settings. Furthermore, current NiCd/NiMH charging techniques generally employ fixed PI or rule-based fuzzy controllers, which are inherently limited in their capacity to accommodate the nonlinear dynamics of batteries. Consequently, a significant research void exists in the formulation of adaptive, AI-driven MSCCC strategies explicitly designed for NiCd and NiMH batteries.

The following is an overview of the main points made by this work:

- Developing a charging system for MSCCC with ANFIS control for the sole purpose of charging the NiCd and NiMH type of batteries.
- Design of smart PFC boost-converter based charger with adaptive current control.
- Performance assessment under the same operating conditions as PI, Fuzzy, and Neural controllers.
- Demonstrate that ANFIS control led to better SoC stability, lower voltage overshoot, and a more graceful current response.
- The proposed charging strategy has been validated with the help of 2-D nickel-based chemistries with simulations done in MATLAB/Simulink software.

2. BACKGROUND

2.1. Multi-stage constant current charging (MSCCC)

Fast charging has emerged as an essential method of getting round the performance and usability limitations of NiCd and NiMH batteries, in high-performance applications such as power tools, in hybrid electric vehicles, and as a backup system. Besides offering the user greater convenience, creating an ingenious and adaptable system of charging is vital in offering higher energy efficiency, reducing the total time of charging, reducing thermal stress, and enhancing the cyclic life of nickel-based battery chemistries. One of the most effective methods of fulfilling these demands is dynamic MSCCC method.

In the MSCCC approach, the conventional CC charging stage is divided into a number of phase, which operate at gradually decreasing currents, or C-rates. Reducing the rate of hydrogen evolution and internal pressure increase that is widespread with NiMH and NiCd cells under constant high-current charging this falling current method also reduces the load on the battery electrodes significantly. Moreover, since it

does not have to use constant voltage stage, the MSCCC method does not overcharge cells and reduces temperature rise and pressure accumulation two effects that reduce the lifetime of sealed NiCd/NiMH cells compared to older methods such as CC constant voltage (CC-CV).

The MSCCC approach has been very popular due to its simplicity, the possibility of connection with real time control systems and the ability to strike a balance between speed and safety. There are many MSCCC frameworks that have been researched in the literature; the frameworks typically comprise between three and ten steps. Each phase has dissimilar transition criteria depending on temperature track, SoC estimations, or voltage levels. The current levels of each stage are also varied as per the type of the battery, the requirements of the application as well as desired performance.

The following performance metrics are usually examined in order to assess how well the MSCCC approach works for NiCd and NiMH batteries,

- Time spent charging
- Efficiency of charging
- Retention of charge/discharge capacity
- temperature increase while charging

By enabling adaptive control over stage currents and switching criteria in real time, AI such as fuzzy controller and PID modelling can further improve MSCCC and produce optimal performance that is suited to battery state and usage conditions.

The primary factor influencing the charging time of NiCd and NiMH batteries is the C-rate of charge; rapid charging is achieved with a greater C-rate. It is, however, possible that the cycle life may be affected if a high C rate is used during charging in terms of thermal stability and charging efficiency. It is worth noting that high current charging for a long duration may be a threat in the middle and high SoC levels; however, NiCd and NiMH are less affected by high current charging compared to lithium-ion batteries.

The increased rate of current may be fully supported by the battery without any adverse effects, especially during the early stages of charging when the SoC levels are less than 40%. This is the stage when electrochemical action is most effective without any prospects for overpressure or thermal stress. On the other hand, internal resistance increases and the danger of polarization effects intensifies as the SoC rises above 50%. This frequently shows up in NiMH cells as the production of oxygen gas at the positive electrode, which, if improperly recombined or vented, can raise internal pressure. It can decrease charge acceptance and worsen the memory effect for NiCd [20].

One of the important metrics for the LIB charging process is how efficiently it charges. The charging efficiency of a LIB is its ability to dissipate energy while charging divided by its capacity to charge. To calculate the charging efficiency, one uses the following (1).

$$\eta(\%) = \frac{I_d \times t_d}{\sum_{i=1}^{n} I_c \times t_c} \times 100 \quad (1)$$

In (1), n, Id, td, Ic, and tc stand for the number of stages, discharging current, discharging time, charging current, as well as charging time simultaneously. A higher C-rate results in a greater capacity loss when charging using the CCCV method. For larger crates, the MSCC charge method is based on the same principle. This method differs from the CCCV technique in that it uses a variable number of charging phases to reduce energy loss. Charging efficiency may be improved by reducing energy loss. Energy loss and charging time might be at odds with one another at times [21]. Although the energy efficiency has decreased by 0.6%, the charging time is decreased by 34% when compared to CCCV utilizing the SoC-based four step charging technique [14]. Energy efficiency is improved with the best possible charge pattern when using the MSCC charging method that incorporates voltage cut-off transition criteria [22].

The charge/discharge capacity is a crucial performance metric for assessing NiCd and NiMH battery charging strategies. The battery's charging capacity is the total amount of charge (measured in Ah) that it can store while being charged. A measure for determining whether charging is complete, the current consumed at the last end, and the ambient temperature is some of the operational elements that affect this capability. At low temperatures (such as 0°C or lower), NiCd and NiMH batteries, for example, usually show decreased charge uptake, which results in undercharging even when the charger is providing current.

Additionally, the total amount of useable energy extracted from the battery throughout discharge is known as the discharging capacity. The discharge performance may be influenced by different factors like internal resistance, SOH, and memory effects. The last one is characteristic for NiCd batteries.

$$\eta_{charge} = \frac{Q_{charge}}{Q_{rated}} \quad (2)$$

$$\eta_{discharge} = \frac{Q_{discharge}}{Q_{rated}} \quad (3)$$

Where,

- Q_{charge}: Actual charge stored during the charging process (Ah)
- $Q_{discharge}$: Actual energy extracted during discharging (Ah)
- Q_{rated}: Nominal (rated) capacity of the battery (Ah)

These normalized values can be used for comparing the performance of the charging strategies, as well as the battery types. This comparison can be particularly useful when considering the impact of AI-optimized MSCCC algorithms under various environmental conditions.

The performance of the NiCd and NiMH types of batteries is directly affected by the increased temperature during charging. Similar to lithium-ion types of batteries, heat is produced internally during charging. This heat is produced due to overpotential effects, as well as ohmic losses. Such heat production occurs particularly when the battery is charged quickly. A considerable amount of heat can be produced during MSCCC charging. This is particularly true when increased levels of current are used during the initial stages of charging. The heat is produced due to Joule heat. The Joule heat can be mathematically expressed as follows,

$$Q_{ohmic} = I_{RMS}^2 \cdot R_{\text{int}} \cdot t \quad (4)$$

Where,

- Q_{ohmic}: Heat generated due to internal resistance (Joules)
- I_{RMS}^2: Root means square value of charging current (A)
- R_{int}: Internal resistance of the battery (Ω)
- t: Charging time (s)

The increasing charging currents during the initial stages of MSCCC lead to an exponential increase in the rate of heat generation, which results in degradation of the electrolyte, increased pressures, and venting issues in sealed NiCd/NiMH batteries. The temperature problems are high in NiMH batteries due to the exothermic reactions that occur during overcharging. This leads to capacity fading, swelling, and rupture of the battery. In order to avoid temperature problems during the charging process, the AI control incorporated in the MSCCC technique helps in monitoring temperature-related charging currents for maintaining temperature levels during the charging process. This ensures the efficiency of the charging process.

2.2. Adaptive neuro-fuzzy inference system (ANFIS)

An international fuzzy system and estimator called ANFIS was suggested by J.S. Roger Jang in 1993. It was based on the Takagi-Sugeno fuzzy model [23]. Using a constant term and linear combination of input parameters, this model creates rule outputs as a Type 3 fuzzy inference system. Final results are obtained by summing together the weighted results of each rule [24]. By combining the best features of artificial neural networks with fuzzy inference systems, ANFIS creates a unified and powerful solution to complex engineering problems [25], [26]. Figure 1 is a schematic representation of the ANFIS architecture. It shows how the system uses neural network learning and fuzzy logic to mimic the input-output interactions of actual systems.

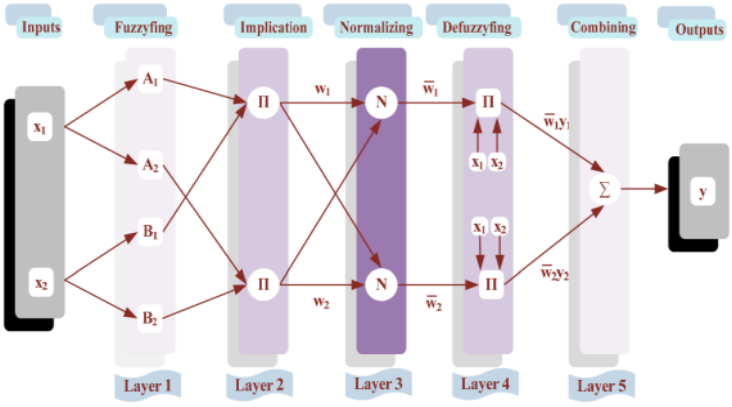

Figure 1. Schematic diagram of the structure of ANFIS [27]

With two inputs (x1 and x2) and one output (y), the basic idea of ANFIS may be expressed as follows.

Rule 1: if x1 is A1 and x2 is B1, then y1=p1 x1+q1 x2+r1

Rule 2: if x1 is A2 and x2 is B2, then y2=p2 x1+q2 x2+r2

The fuzzy set parameters for each input in part-if (permissive portion) are Aj and Bj, while the linear for part then (the succeeding part), the parameters are pj, qj, and rj. There are five distinct levels in the ANFIS architecture for networks with one output and two inputs, the output is computed at the fuzzyification layer, where each node j acts as an adaptable node [28].

$$O_j^1 = \mu A_j(X_1), for\ j = 1 \quad (5)$$

$$O_j^1 = \ for\ j = 3,4 \quad (6)$$

In the Implication Layer, the static nodes denoted by π, function as basic multipliers. The rule firing strength, denoted as wj and computed from the input signals as follows,

$$O_j^2 = \omega_j = \mu A_j(X_1)\mu B_j - 2(X_2), for\ j = 1,2 \quad (7)$$

The normalization layer assigns a fixed node, N, to each node in the network. A signal is produced by dividing the jth rule's firing intensity by the total firing intensities of all rules. w_j for the jth node,

$$O_j^3 = \bar{\omega}_j = \frac{\omega_j}{\omega_1+\omega_2} for\ j\ = 1, \quad (8)$$

Defuzzification layer: In this layer, each adaptive node j includes the arguments (pj, qj, rj, and wj) in its node function. Presented below is the firing strength normalized value,

$$O_j^4 = \bar{\omega}_j y_j = \bar{\omega}_j\left(p_j X + q_j X + r_j\right), for\ j = 1,2 \quad (9)$$

Combination layer: There is just one fixed node in the terminal layer, denoted as ∑, It computes the total end output by adding together all input signals.

$$O_j^5 = \ y = \ \sum_j\left(\bar{\omega}_j y_j\right) = \frac{\sum_j(\omega_j y_j)}{\sum_j \omega_j} \quad (10)$$

3. DESIGN APPROACH

The design of the intelligent charging system involves four major steps: power conversion, boost converter regulation, adaptive controller design, and MSCCC algorithm development. First, the AC input is rectified and fed to the PFC boost converter. Second, the boost converter regulates the DC output with an LC filter to provide low ripple. Third, the ANFIS controller dynamically changes the duty cycle according to the voltage error and system feedback. Finally, the MSCCC algorithm controls the multi-stage current transitions based on the battery's current charge, as illustrated in Figure 2. The charging system's modular architecture enables the coordinated operation of the power stage and the intelligent control stage to provide stable voltage regulation, smooth current supply, and adaptive charging for NiCd and NiMH batteries.

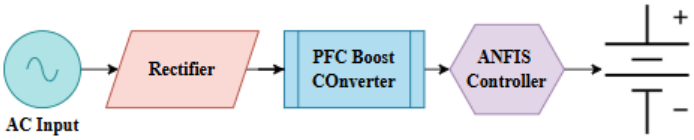

Figure 2. Circuit and control architecture

3.1. Battery specifications

The research investigates NiCd and NiMH battery chemistries often used in high-demand portable and automotive applications. The specified 23.5 Ah of capacity and a nominal voltage of 24V are feasible for

a NiCd battery pack used in a rigorous application. The 49.4 Ah capacity and 25.2V nominal voltage are also appropriate for a NiMH battery pack [29]. All the elements of the control framework and the charger design are selected to conform to these characteristics.

3.2. Use case

The aim is to create an intelligent MSCCC charger architecture that utilizes AI technology and is optimized for better charging efficiency, temperature rise, and battery life. The charger needs to be able to adapt to dynamic changes in the loads and be compatible with both NiCd and NiMH batteries. The control model is simulated using MATLAB Simulink, and a single-input single-output (SISO) adaptive ANFIS controller is executed to enhance control operations in real-time.

3.3. Alternatives and tradeoff's

Although the traditional PI and fuzzy controllers has the benefits of ease of use and little computational complexity are based on fixed parameters and rules, which are not adaptable to the dynamic conditions of the battery. The ANFIS controller adds more complexity to the computations, but this is compensated for by its ability to provide better voltage regulation, smoother current transitions, and better SoC retention. The proposed method does not add to the complexity of the hardware since the ANFIS is at the control level.

3.4. Fundamental battery charging circuit

The suggested charging method employs a single-phase AC source where a diode bridge rectifies the voltage to generate DC input following is lowered by a transformer. A power factor correction boost converter, which controls the charging voltage and raises the input power factor, is supplied by this direct current voltage. The converter is controlled by a controller that includes an ANFIS in accordance with input parameters (voltage, frequency, and phase) and output parameters (battery voltage, SoC).

The charging mechanism used by the system is called the MCCC algorithm. This ensures the charging happens in a specific current stage. The proposed model uses an adaptive neuro fuzzy system to regulate the duty cycle of the boost converter to optimize the levels of voltage and current in real-time according to the SoC of the battery. This ensures the efficient transmission of power without overheating the battery. The controller can switch levels of current to maintain the health of the battery.

4. DESIGN SPECIFICATIONS

In Figure 3, the proposed intelligent MSCCC-based charging system for NiCd and NiMH batteries is designed to ensure high efficiency in charging the batteries with minimum loss of energy, a reduced ripple effect, safe power conversion, and high efficiency. The design parameters for the battery are presented in Tables 1 and 2. The input voltage rectified is represented as Vin, the voltage across the terminals of the battery is represented as VB, the inductor current of the boost converter is represented as IL, and the SoC is the state of the charge of the battery. The proposed charging system is designed to ensure the dynamic charging requirements of the battery with the help of the multistage current profile charging. The proposed charging system is represented as the Power Factor Correction a transformer with adjustable taps, the photoelectric rectifier (PFC) boost converter, and the LC output filter. The basic charging circuit configuration for the proposed charging system for the NiCd and NiMH batteries is represented in Figure 4. The boost converter is designed to ensure the electrical requirements of the NiCd and the NiMH batteries.

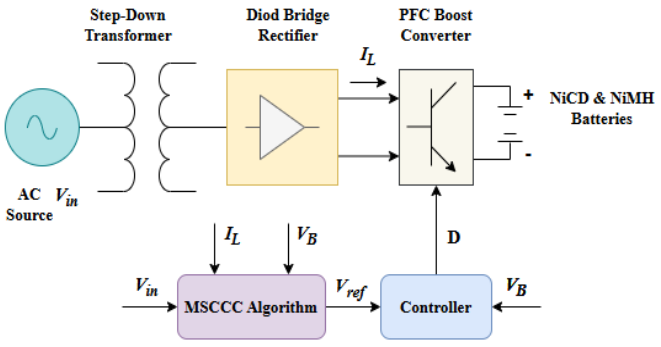

Figure 3. Block diagram of the proposed NiCd and NiMH battery charger with MSCCC algorithm

Table 1. NiMH Parameters

Parameters	Values
Source Voltage	48V
Switching frequency f_s	10e3
Battery specifications	
Nominal voltage	25.2 V
Rated capacity	49.4 Ah
Fully charged voltage	29.6

Table 2. NiCD parameters

Parameters	Values
Source Voltage	48 V
Switching frequency f_s	10e3
Battery specifications	
Nominal voltage	24 V
Rated capacity	49.4 Ah
Fully charged voltage	28.8

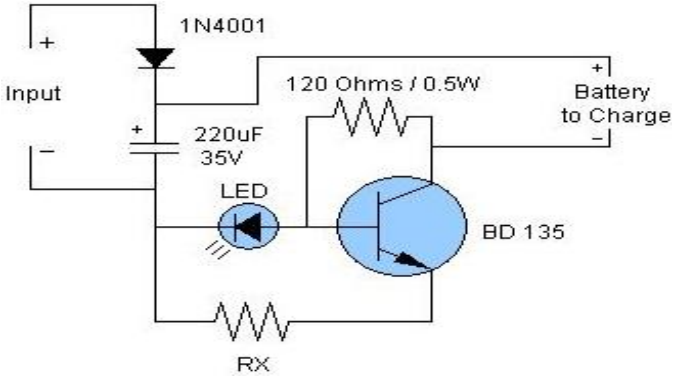

Figure 4. Basic charging circuit with PFC boost converter

4.1. Converter design

The PFC boost converter is of primary importance in controlling the output voltage and input current shape in order to attain a high power factor. An additional LC filter is also provided in the output section in order to eliminate the high-frequency ripple present in the output due to PWM switching. This is not only for voltage regulation but also for battery protection and regularity in charging.

The output voltage of the boost converter, denoted by VB, is given by the following expression based on the duty cycle D(11),

$$V_B = \frac{V_{in}}{1-D} \tag{11}$$

Were,

- V_{in}: Input voltage after rectification
- D: Duty ratio of the PWM signal

To design the inductor, the value of L_{in} is determined using,

$$L_{in} = \frac{V_{in}.D}{f_s.\Delta I_L} \tag{12}$$

Were,

- f_s: Switching frequency of the converter
- ΔI_L: Peak-to-peak ripple current in the inductor

The maximum inductor current, Ipk, is computed as,

$$I_{pk} = \sqrt{2.\frac{p_{in}}{V_{in(\min)}}} \tag{13}$$

Where,

- P_{in}: Input power
- $V_{in(min)}$: Minimum input voltage level

To ensure output voltage stability, the minimum required capacitance Co at the output is given by,

$$C_{O(\min)} = \frac{I_{OUT(\max)}.D}{f_s.\Delta V_B} \tag{14}$$

Where,

- $I_{OUT\ (max)}$: Maximum output current
- ΔVB: Allowable output voltage ripple

The values of these components are very important for the proper functioning of the system in all phases of the MSCCC method with the reduction of switching loss and thermal stress while maintaining the required voltage and current profiles. Accurate adjustment of these parameters guarantees optimum performance during the ANFIS-regulated dynamic charging of both NiCd and NiMH batteries.

4.2. Controller design

A smart MSCCC-based charging architecture relies on a controller to dynamically regulate charging current, output voltage, and power factor of the input AC supply. It incorporates an ANFIS, or adaptive neuro-fuzzy inference system, allows for decisions to be made in real-time based on system feedback and battery status. The controller guarantees optimum performance and safety by adjusting to fluctuating circumstances during each phase of the MCCC process. The controller depends on three essential metrics for proper operation:

- Battery output voltage (V_B): continuously monitored to maintain it at the desired reference value Vrefin each stage of charging.
- AC input voltage (V_{in}): monitored on the transformer's secondary side to coordinate the current through the inductor and keep the phases aligned for PFC.
- Average inductor current (I_L) monitored on the transformer's secondary side to coordinate the current through the inductor and keep the phases aligned for PFC.

4.2.1. Voltage control loop

The outer loop controls voltage at the terminals of the battery. It compares the actual voltage of the batteries with the specified reference voltage (V_{ref}), which is established according to the current charging stage (I_1, I_2, I_3) and the battery's SoC. A proportional-integral (PI) controller manages the resulting voltage error and generates a reference current signal. This instruction is sent to the inner loop to dynamically configure the charging profile. The ANFIS controller improves the performance of the PI action by adaptively modifying the parameters based on the battery behavior that has been learnt**.**

4.2.2. Inner-current loop

An inductor's current is guaranteed by the inner loop to be boost converter, *IL*, closely adheres that the outer loop generates as a reference current. A voltage waveform that is inputted is normalized to unit magnitude and multiplied by the reference current to produce a modulated current signal. The signal is juxtaposed using the actual inductor current *IL*, and another PI controller handles the resulting mistake. This PI controller's output calculates the PWM duty cycle δ, which is then sent to the pulse generator to activate the PFC boost converter's switch. This control ensures that the input current is synchronised with the input voltage, obtaining a near-unity power factor and optimizing efficiency. ANFIS further optimizes the system by persistently adjusting the control surface in response to real-time operational circumstances, internal resistance changes, and SoC variations of the NiCd and NiMH batteries.

5. STATE FLOW CONTROL ALGORITHM

Figure 5 shows that the controller consists of a primary current-control loop and a secondary voltage-control loop. The standard CC-CV approach is compared to the multistage charging process is faster and more effective. It employs a three-step charging process, whereby each stage utilizes distinct current values. Upon initiation of charging, the maximum current is delivered up until the point when the voltage of the battery hits its peak, after which it is drastically lowered with its secondary stage value due to the reduction in current.

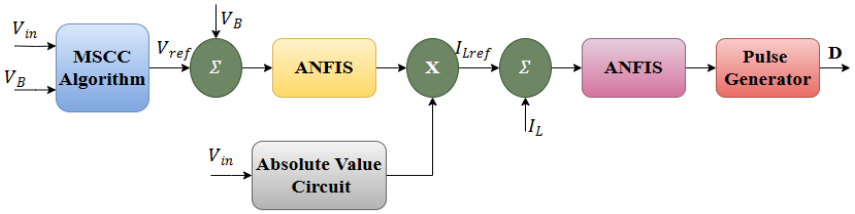

Figure 5. Block diagram of the charge controller

When the current is lowered again, the voltage rises to its maximum. Multistage charging works in this way. Three different values for the charging current are chosen for the three phases. In CC mode, the first

step is to maintain a consistent value for the battery's maximum allowable current (I_1). The final stage current (I_3) is now the only factor that determines the charged AH capacity. The charged capacity increases as the value of I_3 decreases. At now, the time required to charge is determined by selecting both I_1 and $I_3$is solely dependent upon I_2. Consequently, varying values of I_2 will provide different charging durations; nevertheless, the ampere-hour capacity charged will be nearly equivalent to that of I_3. The optimal value of I_2 is determined by means of the following equation:

$$I_2 = \sqrt{I_1 \times I_3} \tag{15}$$

The controller receives a voltage reference from this control circuitry and uses boost PFC to manage the battery current. Figure 6 shows the charging time as a function of the charging current I2, which leads to the optimal value of I2. When I3 is minimised, the overall charging time T is maximized is determined by (3), and the best value is not influenced by Req and Ceq, but rather relies on the values of I1 and I3. During the computation of I2, the values of I1 and I3 are held constant. According to that equation, the shortest amount of time to charge is equal to the value of I2. Here we go into more detail on the thorough MSCC formulation, which can be seen in Figure 7.

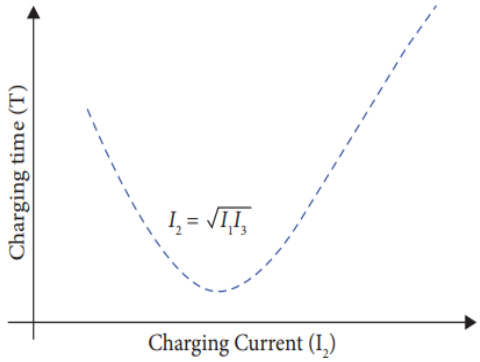

Figure 6. Relationship between charging time (T) and charging current (I2)

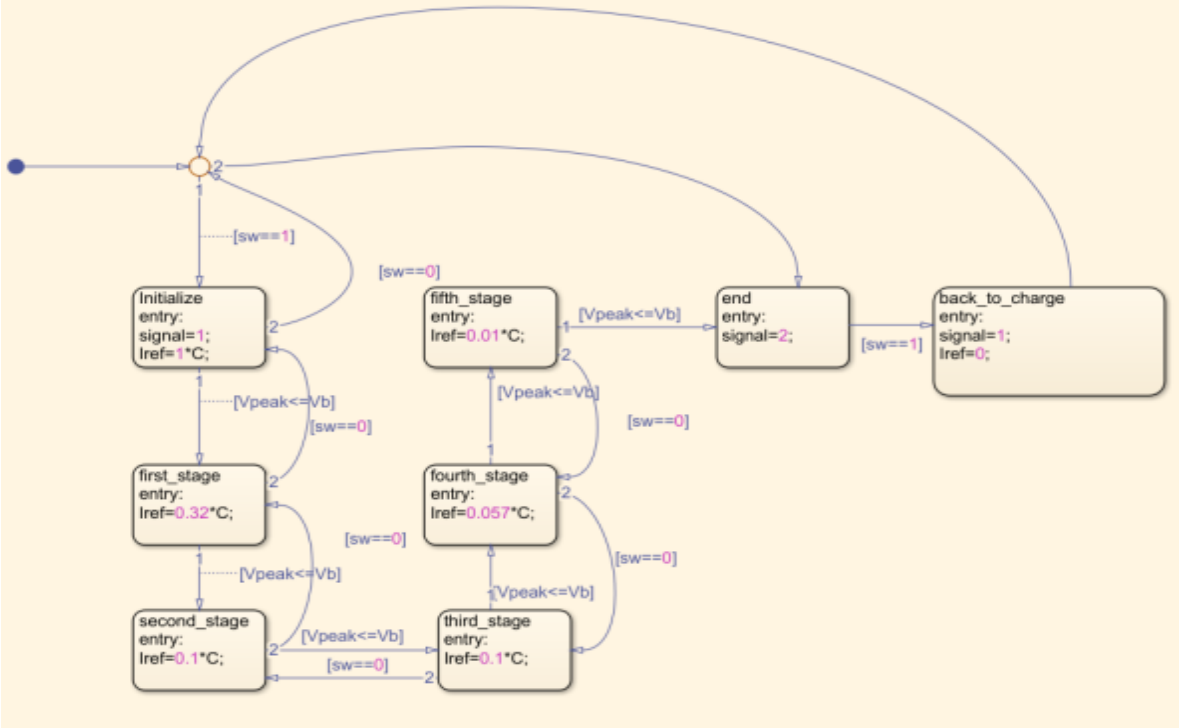

Figure 7. State flow control logic of the multistage current control charging algorithm

5.1. State flow chart demonstration

The proposed ANFIS-based MSCCC charging system for NiCd and NiMH batteries employs a state flow algorithm that starts charging in the first stage with the maximum constant current $I1$, establishing a voltage reference of roughly 35 V. A delay of 0.4 seconds is implemented utilising two consecutive logic blocks to avert the premature activation of future stages caused by the first voltage spike. In the second stage, the reference current diminishes to I2, during which the battery voltage escalates and nears its maximum value of around 29.33 V. Upon the fulfilment of the requirement $Vpeak \leq VB$, the system advances to this phase with an updated reference voltage of 28.25 V. in order to manage transient delays during the voltage, decrease and prevent stage omission, a 1-second delay is similarly included utilizing dual logic blocks. Upon attaining the peak voltage in the third stage, the reference current decreases to $I3$, and charging proceeds under regulated circumstances. Upon reaching and maintaining the peak voltage, the system concludes the charging process by lowering the reference voltage to 0 V, therefore ceasing the current delivery and assuring the safe disconnection of the battery from the charging source.

6. SIMULATION RESULTS AND DISCUSSION

These findings show the results of extensive simulations that were run to evaluate how well a MSCCCF strategy augmented with AI techniques to enhance the charging efficiency of NiMH and NiCd batteries. In addition to that, a simulation study was also performed to compare the performance of conventional charging controllers with the proposed MSCCC incorporating AI technology for important parameters like duration of charging time, thermal stability, retention, and voltage regulation under various operating conditions. This simulation findings to evaluate the efficiency of the suggested MSCCC battery charger based on the ANFIS standard for use with NiCd as well as NiMH batteries. The show is compared with the conventional PI, Fuzzy, and Neural controllers based on important parameters such as charging dynamics, SoC retention, voltage regulation, and current stability. The simulation results clearly show that ANFIS provides a SoC retention value that is 5-8% higher and a voltage overshoot value that is about 20% lower than the PI controller.

6.1. Simulation results for NICD

The Figure 8 illustrates an Adaptive SISO system that is used to enhance the ANFIS training technique, which stands for Neuro-Fuzzy Inference System, charging efficiency of NiCd batteries. Two variables, error and actual plant output, are input to the ANFIS system, and one variable, adjustment to the PI controller, is output. Ten iterations of training are performed until convergence is achieved.

The training has three phases: input1 =-15.3, input 2 = -24.6, and output = -172. In the first part, we see 12 membership functions for the primary input variable, shown as individual lines. Following this, you'll see a description of the 11 membership functions used by the second input variable; MATLAB's ANFIS editor makes these adjustments automatically. In the third stage, the ANFIS system's fuzzy set is shown. Each plot in the training technique depicts a different phase in the educational process. The input data is shown on the x-axis, while the corresponding output values are represented on the y-axis. You can see how the training process affected the output values and membership functions in the charts. The surface topology indicates specific areas of control intensity, illustrating the system's adaptive behavior across the input space. This visualization demonstrates that the ANFIS model has successfully acquired the capability to provide intelligent control outputs, hence improving NiCd battery charging performance inside the MSCCC framework. The simulation outcomes of NiCD are depicted in below given figures.

Figure 9 indicates the change in the SoC of the NiCd battery during a 20 s simulation cycle of four controllers, i.e. ANFIS, Neural, FUZZY and PI. Every controller seeks to maintain SoC at constant, although the PI controller decays faster and then recovers slower. ANFIS is able to maintain a somewhat higher SoC through, which means a greater efficiency and charge retention. FUZZY and Neural lie on the middle ground between these extremes with FUZZY giving a smoother transition and Neural giving a a little sharper one.

Figure 10 will show the profile of battery and supply current under the same controllers. PI controller generates huge abrupt current swings when responding to changes in loads, and ANFIS, Neural, and FUZZY generate more controlled current traces. ANFIS is the most gradual of the intelligent controllers and has low overshoot, which implies better damping and less electrical stress.

Comparison of voltage outputs is made in Figure 11. The PI controller displays huge unexpected peaks and dips indicating reduced stability in voltage. Comparatively, ANFIS and FUZZY have a smaller and more stable voltage band with lesser overshoot. ANFIS demonstrates the most favorable damping and flexibility and offers better consistency in regulation of voltage in the process of changes.

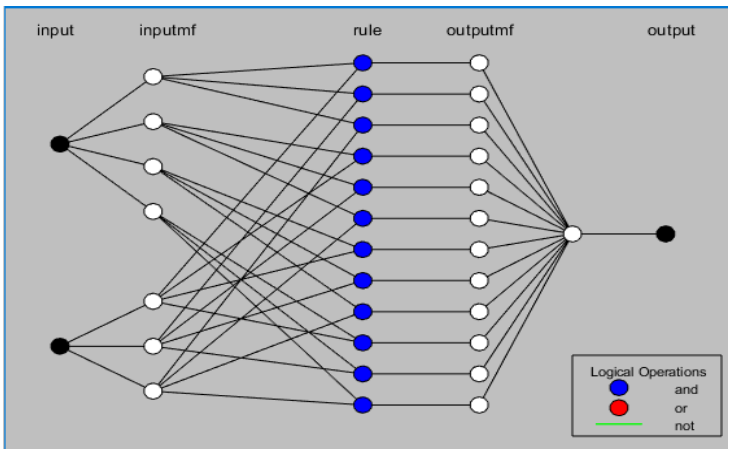

(a)

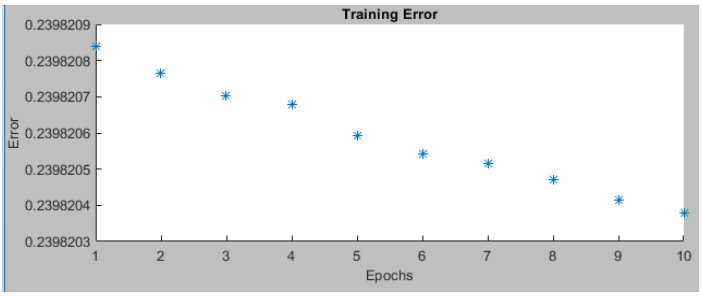

(b)

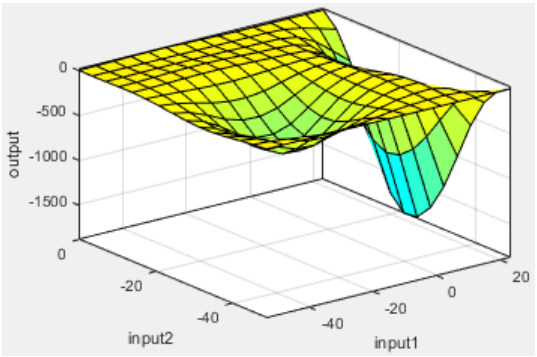

(c)

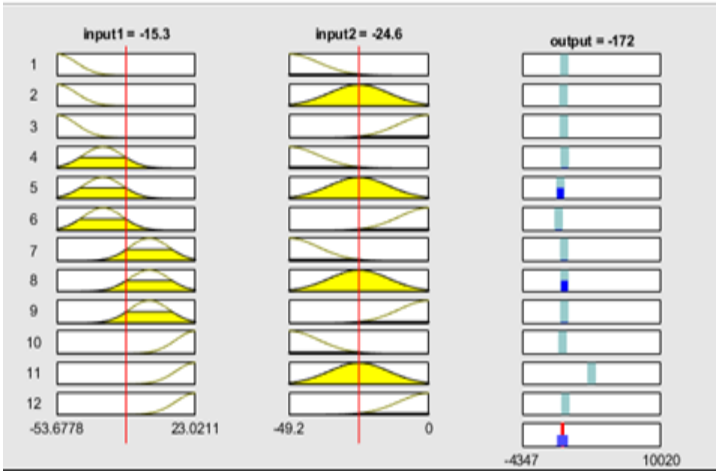

(d)

Figure 8. Training of ANFIS for NICD

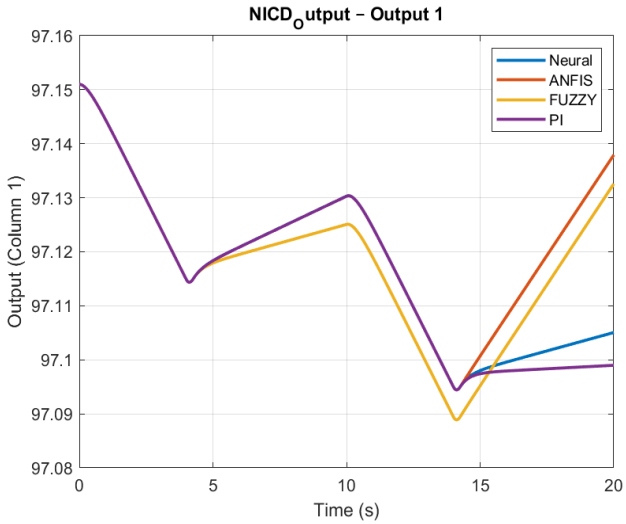

Figure 9. Comparison of NiCd battery SoC under PI, fuzzy, neural, and ANFIS controllers

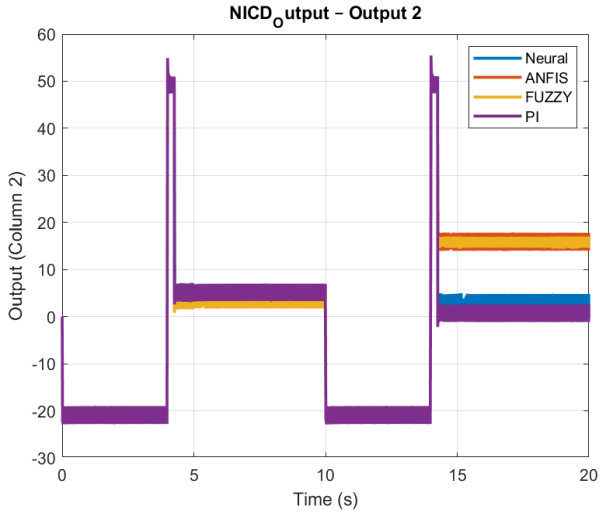

Figure 10. Comparison of battery and supply current for NiCd batteries under different controllers

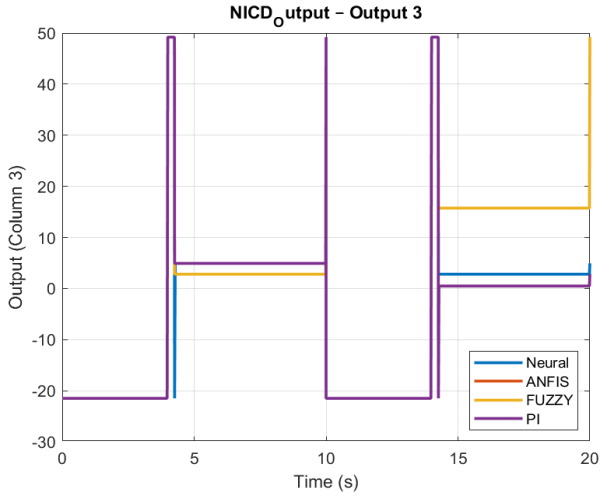

Figure 11. Comparison of max voltage and direct voltage for NICD batteries

The response of the output to the changes in the state of the system is shown in Figure 12. PI controller has a constant flat rate whereas ANFIS, fuzzy and Neural have minor adjustals. Such fine modulations are a pointer to active fine-tuning, which might be influenced to perform better at different loads. Figure 13 shows the highest level of inertia of all the scenarios the results are that all the controllers are essentially maintaining a constant level. ANFIS and fuzzy, nevertheless, are not without adaptive corrections, which are manifested in their capacity to remain adaptive even in steady conditions

In all the products, intelligent controllers, most prominently ANFIS, are always more successful than the PI controller in terms of SoC retention, current stability, voltage regulation and flexibility. While PI control is stable, its lack of flexibility leads to larger overshoots and higher energy loss. ANFIS stands out for balancing energy efficiency, smooth transient response, and adaptive control, validating its effectiveness for NiCd battery management.

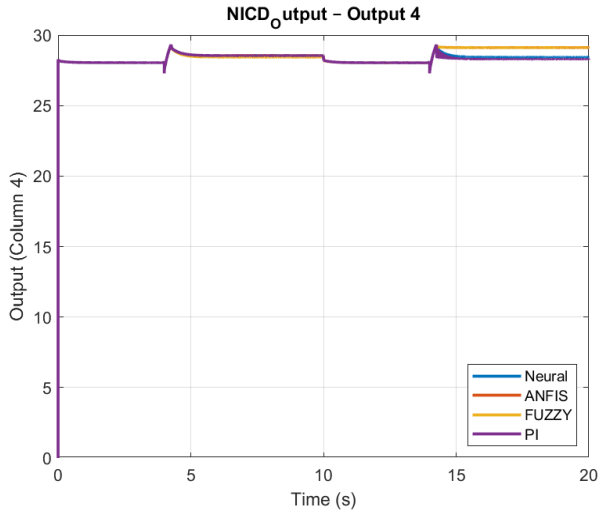

Figure 12. Comparison of PI Controllers for NICD

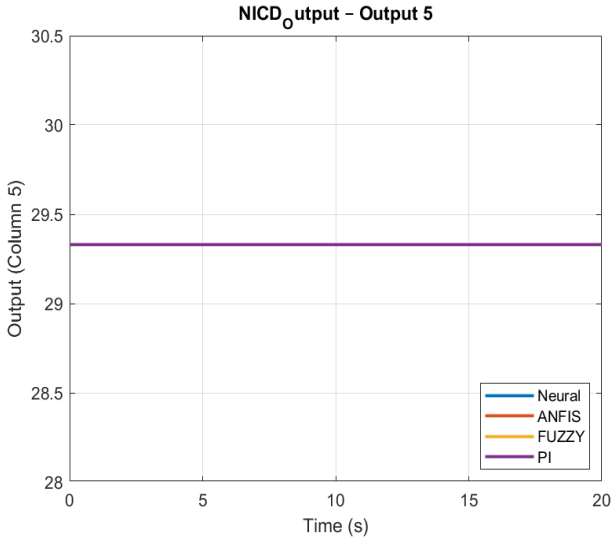

Figure 13. Comparison of PI Controllers for NICD

6.2. Simulation results for NIMH

Figure 14 shows the training process for the ANFIS and NiMH battery. Figure 14(a) displays the first input's membership functions. Figure 14(b) offers the second input's membership functions. The resultant control surface is shown in Figure 14(c), and Figure 14(d) displays the characteristics of the training convergence.

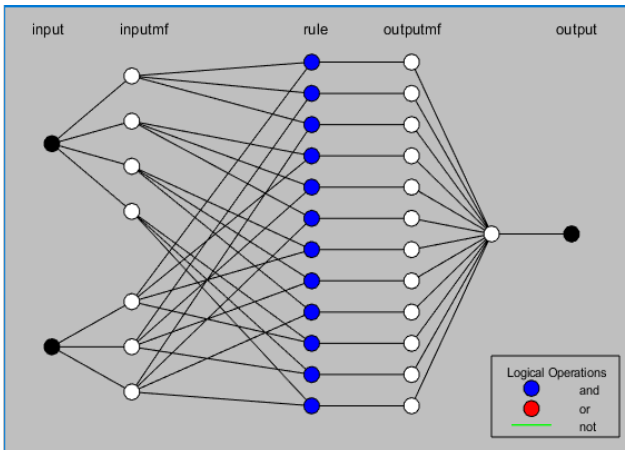

(a)

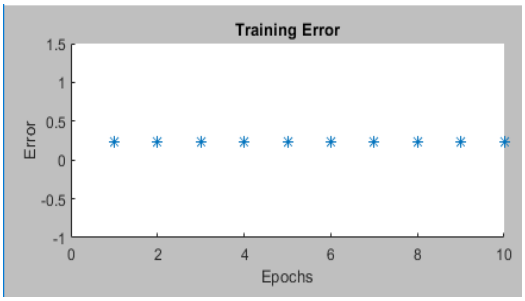

(b)

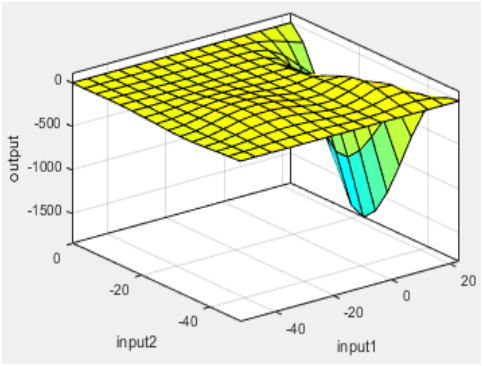

(c)

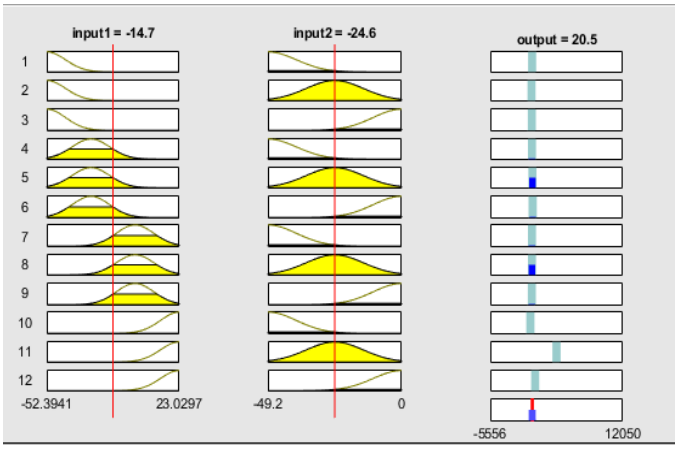

(d)

Figure 14. Training of ANFIS for NIMH

The Figure 14 illustrates an adaptive SISO system known as ANFIS is trained to enhance the charging efficiency of NIMH batteries. The ANFIS system receives two input variables-error and actual plant output-and one output variable-adjustment to the PI controller. Ten epochs of training are conducted until convergence is reached. Three stages comprise the training: input1 = -14.7, input2 = -24.6, and output = 20.5.

The 12 membership functions for the primary input variable are shown in the first stage, each of which is represented by a distinct curve. Eleven functions that are automatically calibrated by the MATLAB ANFIS editor are included in the second phase, which delineates the membership functions to the secondary input variable. The fuzzy set of the ANFIS system is presented in the final step. The training process is demonstrated by a sequence of plots, each illustrating a distinct phase of the learning process. The x-axis represents the input data, and the y-axis denotes the corresponding output values. From these graphs, one can get an idea about the membership functions and output value during the training process. The visual representation provides a clear idea about the capabilities of the ANFIS model in learning from the input data and generating the optimal charging response for the efficient management of the NiMH battery charging using the proposed MSCCC method. The simulation results for the NiMH battery are shown in the figures provided below.

Figure 15 illustrates the SoC change of NiMH battery during a 20s simulation under ANFIS, Neural, fuzzy and PI. The controllers are all heading in the same direction that is towards the decline but PI has the lowest SoC that indicates that it consumes more energy. ANFIS has the best SoC in the entirety, meaning that it has high energy retention. The next to come after ANFIS with minor adjustments to SoC stability are fuzzy and neural.

Figure 16 represents the character of current battery and supply at various loads steps. PI controller indicates high step variations on the current at the switching points compared with ANFIS, Neural and fuzzy which exhibit a smooth response. The intelligent controllers have the most balanced profile that ANFIS; the overshoot is minimal, the transitions are stable, which indicates that the transient changes in loads are more readily damped as well as the control of the same.

Comparison of voltage responses is made in Figure 17. PI produces jump-up and abrupt fluctuation in load changing voltages. Fuzzy and Neural transitions slower than ANFIS which has most controllable voltage behavior with low spikes and rapid settling and therefore can better control the voltage dynamics.

Figure 18 shows the steady-state output inclining towards 30 units. PI control will show a straight line with minimal variations between switching points, whereas ANFIS, fuzzy and Neural will display minor adaptive variations, which will represent fine-tuning about the setpoint. This adaptive process can bring a perturbation to a stability level that is small.

In constant conditions, this is observed in Figure 19 whereby there is constant output regulation. The value difference of all the controllers is of the order of 29.3 units, yet the variations are not significant and could be imperceptible. Though on this scale ANFIS and fuzzy look like PI in terms of their visual aspect, they do not lose their fluidity capabilities, and this can turn out to be handy in more dynamic scenarios.

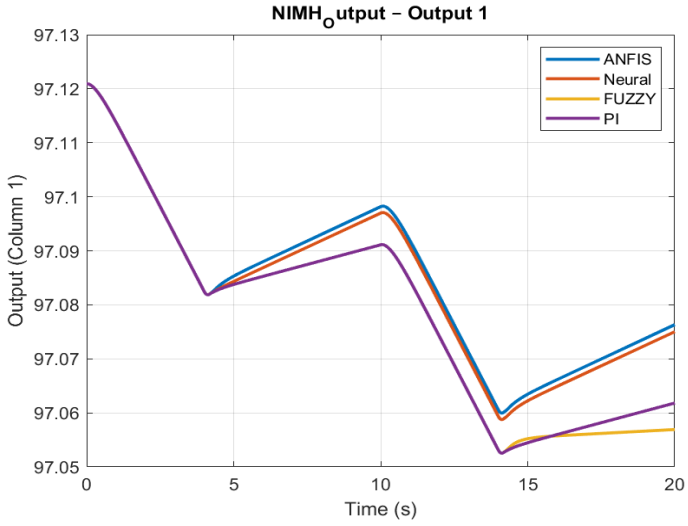

Figure 15. SoC variation of NiMH battery under PI, fuzzy, neural, and ANFIS controllers

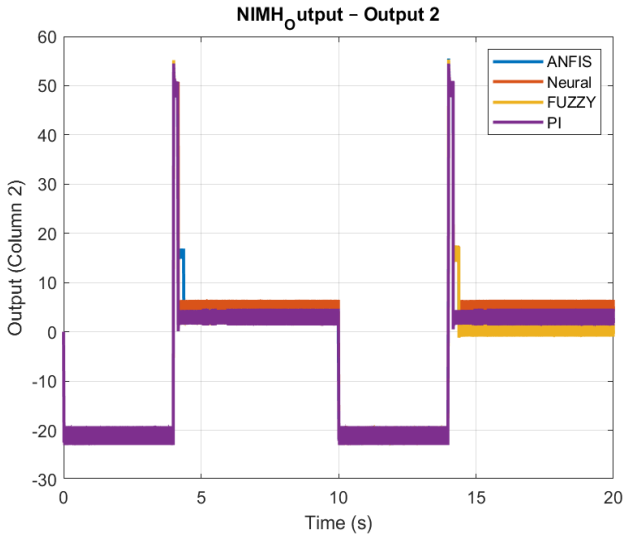

Figure 16. Comparison of battery and supply current for NIMH

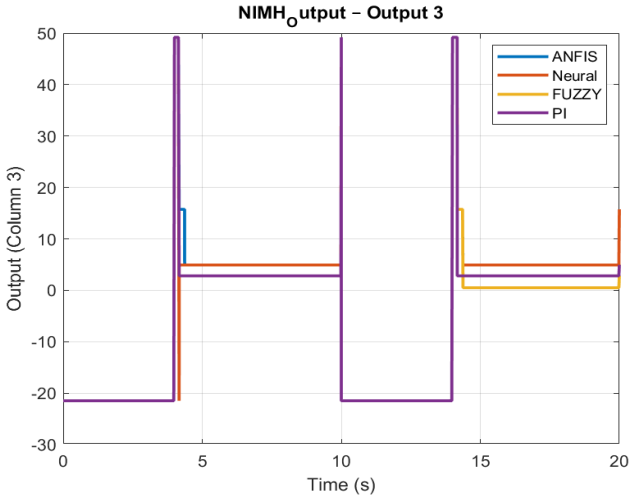

Figure 17. Comparison of max voltage and direct voltage for NIMH

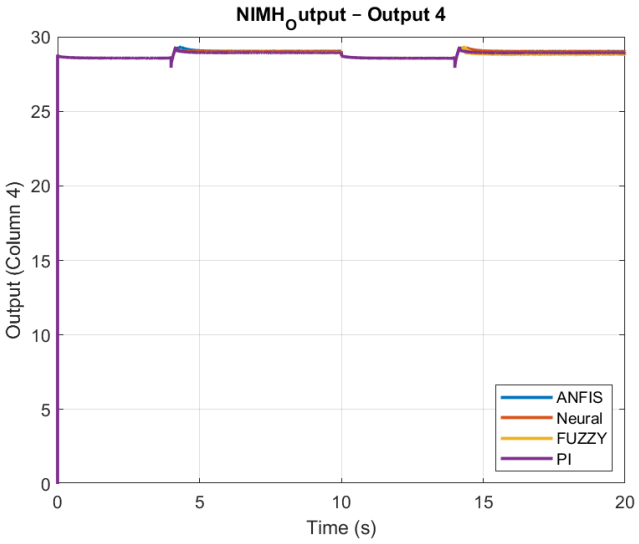

Figure 18. Comparison of PI controllers for NIMH

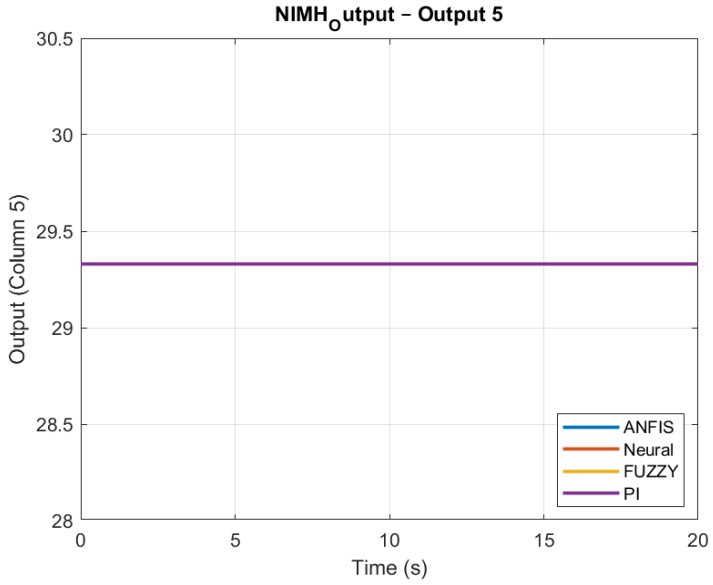

Figure 19. Comparison of PI controllers for NIMH

Overall, during SoC, current, voltage, and steady-state operation, smart controllers, and specifically, ANFIS are reliable to provide a superior regulation and sweeter transient and efficient energy consumption as compared to the traditional PI controller. In the vast majority of cases, which ANFIS proves to be the most stable, fuzzy and Neural methods are also better than PI.

7. DISCUSSION

According to the simulation data, there is no doubt that the proposed AI-enhanced the MSCCC technique effectively increases the efficiency of the charging of both NiCd and NiMH batteries. The ANFIS can be useful in the control of the dynamic charging parameters in question and achieve better control of battery current, voltage regulation, and SoC stability. The ANFIS controller of NiCd batteries was automatically able to achieve a better SoC, smaller changes in voltage and allowed a more balanced transition of current flows in comparison to the fuzzy and traditional PI controllers. ANFIS was found to adapt better to changes in load in NiMH systems leading to optimal charge retention, reduced thermal load, and improved steady-state accuracy. Such benefits are particularly crucial because of temperature sensitivity and ageing behavior of Ni based chemistries.

The superior adaptive capability and control accuracy of ANFIS as compared to the nonlinear battery dynamics of the state-of-the-art control strategies can be explained by the fact that ANFIS represents a hybrid learning-inference framework, thus being able to adapt continuously to nonlinear battery dynamics. Unlike PI and fuzzy controllers, which rely on a fixed gain or a set of fixed rules, ANFIS changes its control area on real-time data. These advantages are reduced overshoot, better damping of current oscillations, and enhanced SoC stability of both NiCd and NiMH batteries, compared to the traditional PI and fuzzy controllers, which relies on fixed parameters or the pre-determined rule bases. The ANFIS controller learns the nonlinear dependence between voltage error and control action dynamically, as opposed to the traditional PI and fuzzy controllers. The adaptive learning capability of ANFIS will help it respond to variations in battery internal resistance, SoC and load disturbances.

The findings of the simulation show that PI control exhibits bigger voltage overshoot and abrupt changes in current, as compared to fuzzy and neural controllers, which provide moderate improvements. On the other hand, ANFIS always yields smoother current transitions, reduced overshoot and improved SoC retention. Such advantages are attributed to the fact that it integrates learning and reasoning architecture hence justifying its suitability when it comes to intelligent MSCCC applications. The obtained results in the terms of charging stability and SoC retention have great implications in the area of electric mobility, power tools and energy storage of the backup power system, where nickel-based batteries are still used. The increased voltage overshoot reduction and current profiles enhance the reduction of the electrical and thermal stress, thereby increasing battery life.

8. CONCLUSION

This study addressed the less used adaptive AI techniques to charge NiCd and NiMH batteries by presenting a MSCCC system based on ANFIS. This study shows the effectiveness of integrating the ANFIS-based AI in the MSCCC-charging system of NiCd and NiMH batteries, unlike the conventional PI and fuzzy-controlled charging systems, which apply fixed parameters, which lead to a significant change in energy efficiency, thermal regulation and charge stability. The real-time feedback-based AI approach adjusts the charging parameters dynamically, outperforming the conventional PI, Neural and fuzzy logic control on such important performance indicators like current control, voltage stability, and SoC maintenance. The MSCCC architecture, built on ANFIS, helps to extend battery life and safety, minimize waste of energy and temperature buildup at the expense of enhancing adaptive responsiveness to operating conditions that vary. The proposed intelligent control system will be a practical and scalable answer to complex battery charging in high-demand environments, and may be adapted to different battery chemistries in the future and be implemented in practice.

The study has a number of limitations in spite of the developments as follows; the current research work is confined to the simulation-based validation. Despite the fact that the findings prove the effectiveness of the proposed ANFIS-MSCCC method, the robustness is to be tested practically. It will be possible to work on laboratory-scale validation on actual NiMH battery packs, integration of IoT-based monitoring to predictive maintenance, and generalizing the proposed framework to hybrid battery systems in the future. Achievement of ANFIS training and real-time embedded implementation will also be experimented on to be further optimized.

ACKNOWLEDGMENT

The authors gratefully acknowledge the Department of Electrical Engineering, Madan Mohan Malaviya University of Technology, for their invaluable support, technical guidance, and research infrastructure that contributed significantly to the successful completion of this study.

FUNDING INFORMATION

This research received no specific grant from any funding agency in the public, commercial, or not-for-profit sectors.

AUTHOR CONTRIBUTIONS STATEMENT

This journal uses the Contributor Roles Taxonomy (CRediT) to recognize individual author contributions, reduce authorship disputes, and facilitate collaboration.

Name of Author	C	M	So	Va	Fo	I	R	D	O	E	Vi	Su	P	Fu
Somendra Banerjee	✓	✓	✓	✓	✓	✓		✓	✓	✓	✓		✓	
Awdhesh Kumar		✓				✓	✓			✓	✓	✓		
Vinod Kumar Giri	✓		✓	✓			✓			✓	✓	✓		

C : **C**onceptualization
M : **M**ethodology
So : **So**ftware
Va : **Va**lidation
Fo : **Fo**rmal analysis
I : **I**nvestigation
R : **R**esources
D : **D**ata Curation
O : Writing - **O**riginal Draft
E : Writing - Review & **E**diting
Vi : **Vi**sualization
Su : **Su**pervision
P : **P**roject administration
Fu : **Fu**nding acquisition

CONFLICT OF INTEREST

The authors declare that there is no conflict of interest regarding the publication of this research work.

DATA AVAILABILITY

No significant external datasets were utilized in this study. All relevant simulation data and methodological details have been appropriately declared within the manuscript.

REFERENCES

[1] A. Barré, B. Deguilhem, S. Grolleau, M. Gérard, F. Suard, and D. Riu, "A review on lithium-ion battery ageing mechanisms and estimations for automotive applications," *J. Power Sources*, vol. 241, pp. 680–689, 2013, doi: https://doi.org/10.1016/j.jpowsour.2013.05.040.

[2] M. V Micea, L. Ungurean, G. N. Cârstoiu, and V. Groza, "Online State-of-Health Assessment for Battery Management Systems," *IEEE Trans. Instrum. Meas.*, vol. 60, no. 6, pp. 1997–2006, 2011, doi: 10.1109/TIM.2011.2115630.

[3] M. V Micea, G. N. Carstoiu, L. Ungurean, D. Chiciudean, V.-I. Cretu, and V. Groza, "PARSECS: A Predictable Data Communication System for Smart Sensors and Hard Real-Time Applications," *IEEE Trans. Instrum. Meas.*, vol. 59, no. 11, pp. 2968–2981, 2010, doi: 10.1109/TIM.2010.2046363.

[4] J. C. Viera, M. Gonzalez, J. C. Anton, J. C. Campo, F. J. Ferrero, and M. Valledor, "NiMH vs NiCd Batteries under High Charging Rates," in *INTELEC 06 - Twenty-Eighth International Telecommunications Energy Conference*, 2006, pp. 1–6. doi: 10.1109/INTLEC.2006.251592.

[5] J. Diaz, J. A. Martin-Ramos, A. M. Pernia, F. Nuno, and F. F. Linera, "Intelligent and universal fast charger for Ni-Cd and Ni-MH batteries in portable applications," *IEEE Trans. Ind. Electron.*, vol. 51, no. 4, pp. 857–863, 2004, doi: 10.1109/TIE.2004.831740.

[6] M. I. Wahyuddin, P. S. Priambodo, and H. Sudibyo, "Direct current load effects on series battery internal resistance," in *2017 15th International Conference on Quality in Research (QiR) : International Symposium on Electrical and Computer Engineering*, 2017, pp. 120–123. doi: 10.1109/QIR.2017.8168465.

[7] C. Zhao, H. Yin, and C. Ma, "Equivalent Series Resistance-based Real-time Control of Battery-Ultracapacitor Hybrid Energy Storage Systems," *IEEE Trans. Ind. Electron.*, vol. 67, no. 3, pp. 1999–2008, 2020, doi: 10.1109/TIE.2019.2901640.

[8] B. V Ratnakumar, M. C. Smart, L. D. Whitcanack, and R. C. Ewell, "The impedance characteristics of Mars Exploration Rover Li-ion batteries," *J. Power Sources*, vol. 159, no. 2, pp. 1428–1439, 2006, doi: https://doi.org/10.1016/j.jpowsour.2005.11.085.

[9] Y.-H. Liu, C.-H. Hsieh, and Y.-F. Luo, "Search for an Optimal Five-Step Charging Pattern for Li-Ion Batteries Using Consecutive Orthogonal Arrays," *IEEE Trans. Energy Convers.*, vol. 26, no. 2, pp. 654–661, 2011, doi: 10.1109/TEC.2010.2103077.

[10] Y.-H. Liu, J.-H. Teng, and Y.-C. Lin, "Search for an optimal rapid charging pattern for lithium-ion batteries using ant colony system algorithm," *IEEE Trans. Ind. Electron.*, vol. 52, no. 5, pp. 1328–1336, 2005, doi: 10.1109/TIE.2005.855670.

[11] L.-R. Dung and J.-H. Yen, "ILP-based algorithm for Lithium-ion battery charging profile," in *2010 IEEE International Symposium on Industrial Electronics*, 2010, pp. 2286–2291. doi: 10.1109/ISIE.2010.5637639.

[12] P. M. Attia *et al.*, "Closed-loop optimization of fast-charging protocols for batteries with machine learning," *Nature*, vol. 578, no. 7795, pp. 397–402, 2020, doi: 10.1038/s41586-020-1994-5.

[13] C.-H. Lee, T.-W. Chang, S.-H. Hsu, and J.-A. Jiang, "Taguchi-based PSO for searching an optimal four-stage charge pattern of Li-ion batteries," *J. Energy Storage*, vol. 21, pp. 301–309, 2019, doi: https://doi.org/10.1016/j.est.2018.11.031.

[14] C.-H. Lee, M.-Y. Chen, S.-H. Hsu, and J.-A. Jiang, "Implementation of an SOC-based four-stage constant current charger for Li-ion batteries," *J. Energy Storage*, vol. 18, pp. 528–537, 2018, doi: https://doi.org/10.1016/j.est.2018.06.010.

[15] L. Jiang *et al.*, "Optimization of Variable-Current Charging Strategy Based on SOC Segmentation for Li-ion Battery," *IEEE Trans. Intell. Transp. Syst.*, vol. 22, no. 1, pp. 622–629, 2021, doi: 10.1109/TITS.2020.3006092.

[16] S.-C. Wang and Y.-H. Liu, "A PSO-Based Fuzzy-Controlled Searching for the Optimal Charge Pattern of Li-Ion Batteries," *IEEE Trans. Ind. Electron.*, vol. 62, no. 5, pp. 2983–2993, 2015, doi: 10.1109/TIE.2014.2363049.

[17] P. Makeen, H. A. Ghali, and S. Memon, "Experimental and Theoretical Analysis of the Fast Charging Polymer Lithium-Ion Battery Based on Cuckoo Optimization Algorithm (COA)," *IEEE Access*, vol. 8, pp. 140486–140496, 2020, doi: 10.1109/ACCESS.2020.3012913.

[18] G.-J. Chen, Y.-H. Liu, S.-C. Wang, Y.-F. Luo, and Z.-Z. Yang, "Searching for the optimal current pattern based on grey wolf optimizer and equivalent circuit model of Li-ion batteries," *J. Energy Storage*, vol. 33, p. 101933, 2021, doi: https://doi.org/10.1016/j.est.2020.101933.

[19] A. B. Khan and W. Choi, "Optimal Charge Pattern for the High-Performance Multistage Constant Current Charge Method for the Li-Ion Batteries," *IEEE Trans. Energy Convers.*, vol. 33, no. 3, pp. 1132–1140, 2018, doi: 10.1109/TEC.2018.2801381.

[20] F. An, R. Zhang, Z. Wei, and P. Li, "Multi-stage constant-current charging protocol for a high-energy-density pouch cell based on a 622NCM/graphite system," *RSC Adv.*, vol. 9, no. 37, pp. 21498–21506, 2019, doi: 10.1039/c9ra03629f.

[21] Y. Li *et al.*, "Optimization of charging strategy for lithium-ion battery packs based on complete battery pack model," *J. Energy Storage*, vol. 37, p. 102466, 2021, doi: https://doi.org/10.1016/j.est.2021.102466.

[22] L. Jiang *et al.*, "Optimization of multi-stage constant current charging pattern based on Taguchi method for Li-Ion battery," *Appl. Energy*, vol. 259, p. 114148, 2020, doi: https://doi.org/10.1016/j.apenergy.2019.114148.

[23] S. Samantaray, P. Sahoo, A. Sahoo, and D. P. Satapathy, "Flood discharge prediction using improved ANFIS model combined with hybrid particle swarm optimisation and slime mould algorithm," *Environ. Sci. Pollut. Res.*, vol. 30, no. 35, pp. 83845–83872, 2023.

[24] W. Sultana and S. D. S. Jebaseelan, "ANFIS controller for photovoltaic inverter transient and voltage stability enhancement," *Meas. Sensors*, vol. 33, p. 101154, 2024.

[25] S. Kanwal and S. Jiriwibhakorn, "Advanced fault detection, classification, and localization in transmission lines: A comparative study of ANFIS, neural networks, and hybrid methods," *IEEE access*, vol. 12, pp. 49017–49033, 2024.

[26] M. S. Rahman, S. K. Dumpeti, M. Davoodi, and M. H. Ali, "Model Predictive Control for Misalignment Compensation in Dynamic Wireless Charging of Electric Vehicles," *Authorea Prepr.*, 2024.

[27] M. S. Rahman and M. H. Ali, "Adaptive Neuro Fuzzy Inference System (ANFIS)-Based Control for Solving the Misalignment Problem in Vehicle-to-Vehicle Dynamic Wireless Charging Systems," *Electron.*, vol. 14, no. 3, 2025, doi: 10.3390/electronics14030507.

[28] A. Belkebir, Y. Bourek, and H. Benguesmia, "Adaptive Neuro-Fuzzy Inference System Application of Flashover Voltage of High-Voltage Polluted Insulator," *J. Electr. Eng. Technol.*, vol. 19, no. 6, pp. 3839–3849, 2024.

[29] P. A. P. Balamurugan, "State-Flow Control Based Multistage Constant-Current Battery Charger for Electric Two-Wheeler," *J. Adv. Transp.*, 2023.

BIOGRAPHY OF AUTHORS

Mr. Somendra Banerjee is a Research Scholar at the Department of Electrical Engineering, Madan Mohan Malaviya University of Technology, Gorakhpur, India. He received his Master's degree in Engineering from the National Institute of Technical Teachers' Training and Research (NITTTR), Chandigarh, India, in 2012. His research interests include Advanced Control Techniques, Intelligent Control, Power Converters, and Battery Management Systems for Electric Vehicles, and Artificial Intelligence. He has published several research papers on controlling electrical systems using different control techniques, optimization of parameters of electrical systems, and applications of artificial intelligence techniques for optimization. He can be contacted at email: banerjeesomendra83@gmail.com.

Dr. Awadhesh Kumar is an Associate Professor in the Department of Electrical Engineering at Madan Mohan Malaviya University of Technology (MMMUT), Gorakhpur, India. He received his Ph.D. in Electrical Engineering from MNNIT Allahabad in 2017, M.E. in Instrumentation and Control from NITTTR Chandigarh in 2012, and B.E. in Electrical and Electronics Engineering from BIT Mesra, Ranchi, in 1998. His research interests include Control Systems, Model Order Reduction, Controller Design, Nonlinear Control, and the application of Optimization and Artificial Intelligence techniques in control design. He has published more than 30 research papers, supervised 37 M.Tech. theses and 5 Ph.D. dissertations, and has been actively involved in organizing seminars, workshops, and conferences. He has also received awards for excellence in teaching. He can be contacted at email: akee@mmmut.ac.in.

Dr. Vinod Kumar Giri is a Professor in the Department of Electrical Engineering at Madan Mohan Malaviya University of Technology (MMMUT), Gorakhpur, India, where he has served since 1989. He was formerly the Founder Director of Rajkiya Engineering College, Sonbhadra, U.P. India (2016–2021). He received his Ph.D. in Electrical Engineering from the Indian Institute of Technology Roorkee in 2003, M.E. in Measurement and Instrumentation from the University of Roorkee in 1997, and B.E. in Electrical Engineering from REC Surat (now SVNIT), Gujarat, in 1988. His research interests include Renewable Energy Systems (Solar PV), Control Systems, Intelligent Control, Biomedical Signal Processing, and Electrical Machine Modeling. He has published more than 110 research papers and has guided several Ph.D. and postgraduate students. He can be contacted at email: girivkmmm@gmail.com.